Supplementary Information for Rapid Decay of the Native Intermediate in the Metallooxidase Fet3p Enables Controlled Fe^{II} Oxidation for Efficient Metabolism

Stephen M. Jones,[†] David E. Heppner,[†] Kenny Vu,[‡] Daniel J. Kosman,[*,‡] and Edward I. Solomon[*,†]

†*Department of Chemistry, Stanford University, 333 Campus Dr. Stanford, CA 94305*

‡*Department of Biochemistry, The University at Buffalo, 140 Farber Hall, 3435 Main St, Buffalo, NY 14214*

E-mail: camkos@buffalo.edu; edward.solomon@stanford.edu

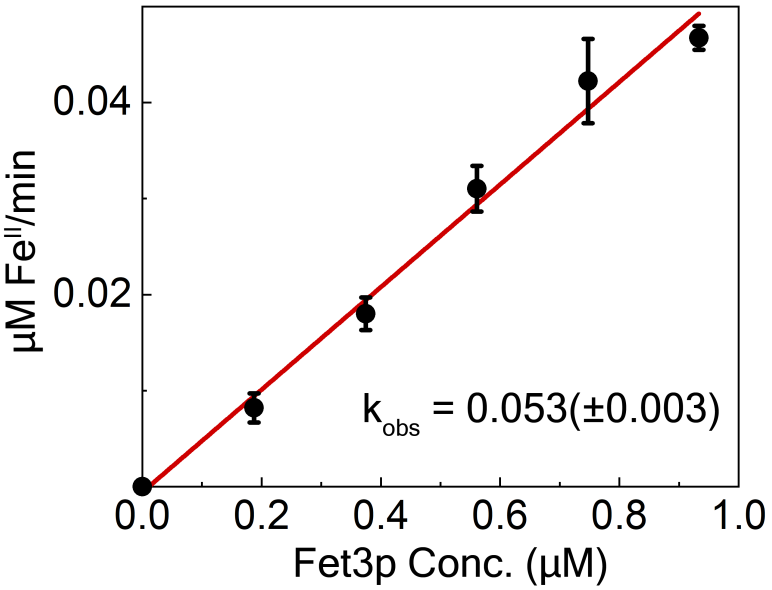

Figure S1: Fe^{II} oxidation kinetics by wild-type Fet3p. Oxidation monitored at 315 nm (ϵ = 2200 $M^{-1}cm^{-1}$) in the presence of atmospheric O_2 and 0–0.93 μM Fet3p.

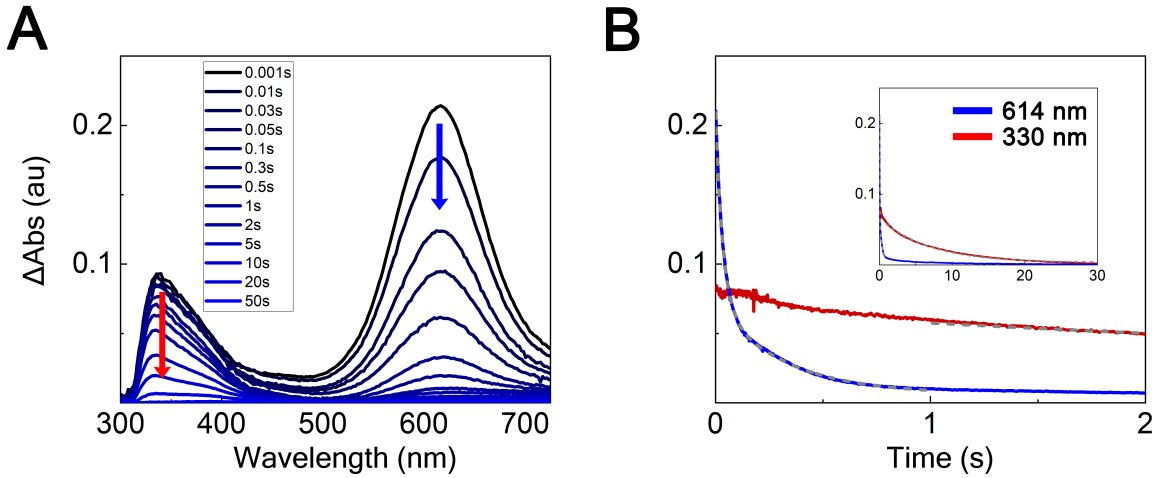

Figure S2: RO reduction in *Rv*L with excess hydroquinone. (A) Selected SF Abs spectra between 1 ms and 50 s after mixing and (B) 330 nm and 608 nm Abs traces over the first 2 s. Inset shows slow 330 nm decay over 30 s. Colored arrows in A correspond to wavelength traces in B with direction of change of Abs features indicated. Fits to 330 nm and 608 nm bands are shown as gray dashed lines with fits described in text. Post mixing conditions: [*Rv*L] = 50 μM, [hydroquinone] = 45.7 mM, pH 7.5, 4 °C.

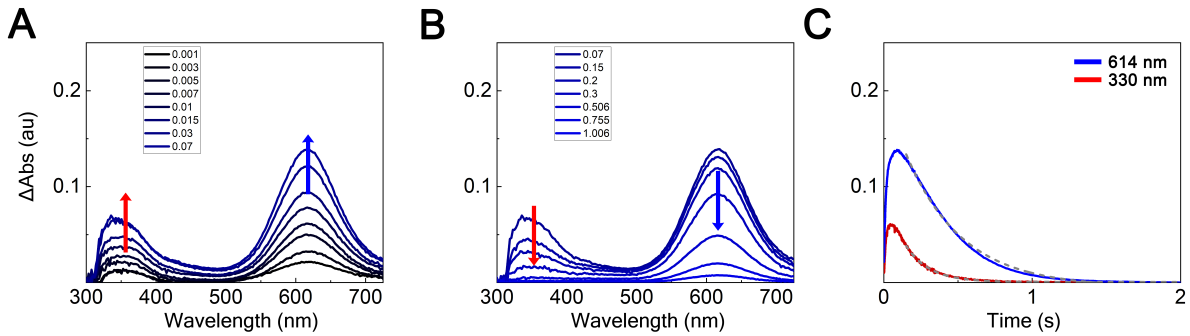

Figure S3: NI reduction in *Rv*L with excess hydroquinone. (A) Selected SF Abs spectra between 1 ms and 70 ms after mixing, (B) SF Abs spectra from 70 ms to 1 s and (C) Abs traces of 365 and 608 nm intensity. Colored arrows in A and B correspond to wavelength traces in C with direction of change of Abs features indicated. Fits to both 330 nm and 608 nm bands are shown as gray dashed lines with fits described in text. Post mixing conditions: [*Rv*L] = [O_2] = 50 μM, [hydroquinone] = 42 mM, pH 7.5, 4 °C.

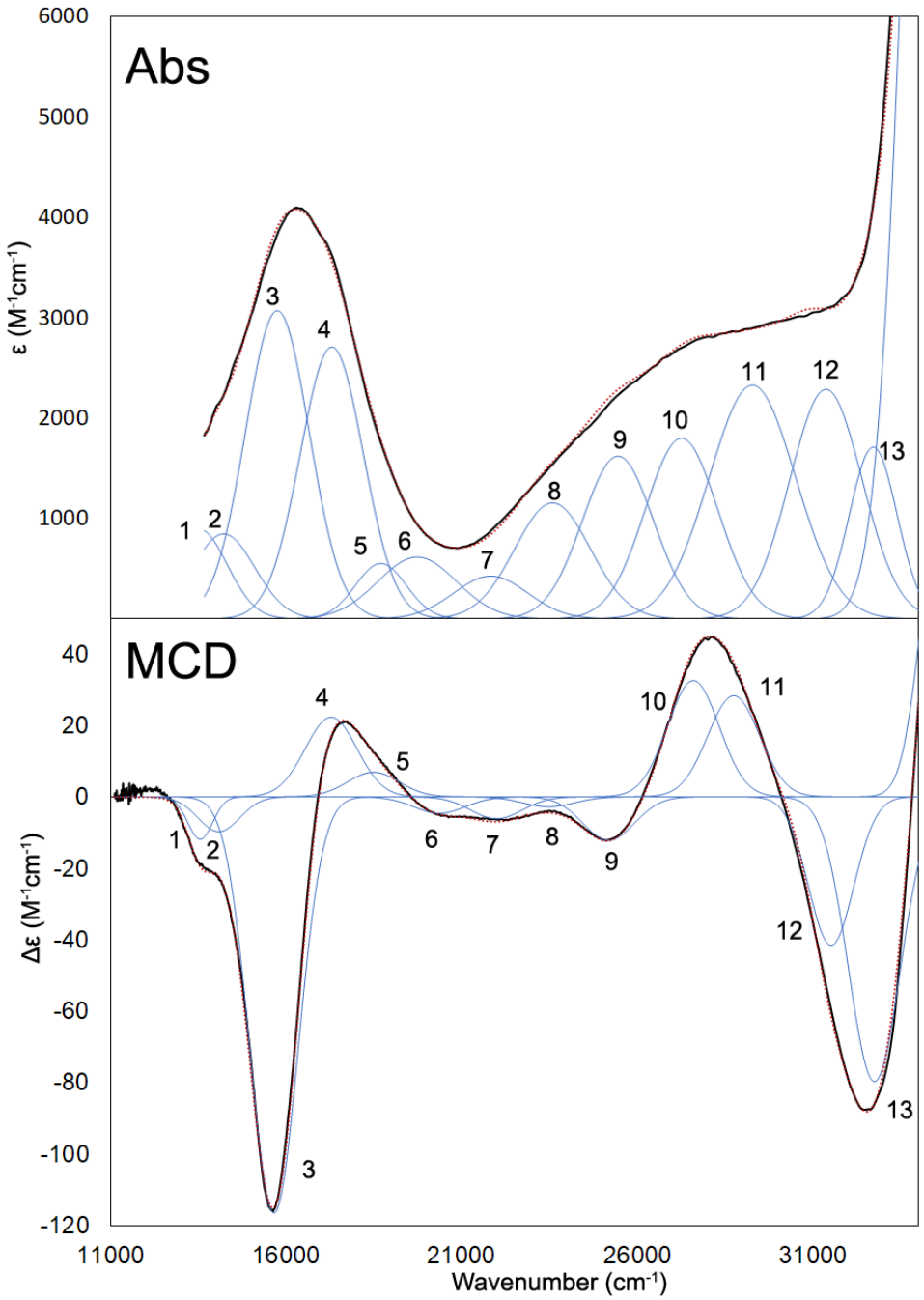

Figure S4: UV-Vis Abs and MCD spectra (7 T, 5 K) of NI in Fet3p. Bands 1-13 were simultaneously fit with parameters given in Table S2

.

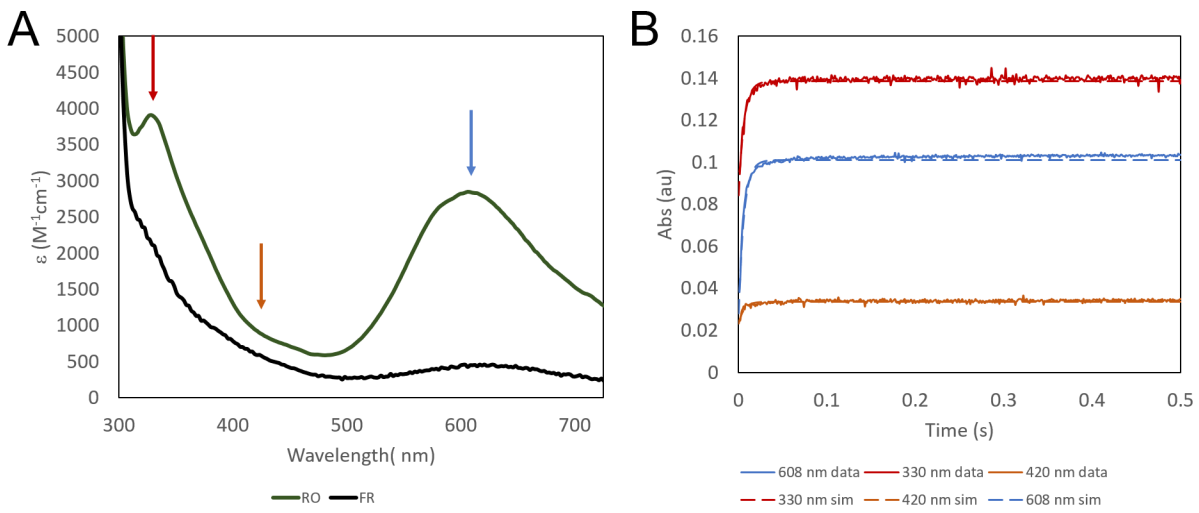

Figure S5: Extracted SVD spectra of RO and FR (A) and fits to 330, 420, and 608 nm traces (B) of SF Abs data for O_2 reaction with FR Fet3p at pH 6. Data at this pH could be adequately modeled as FR→ RO without inclusion of an NI.

.

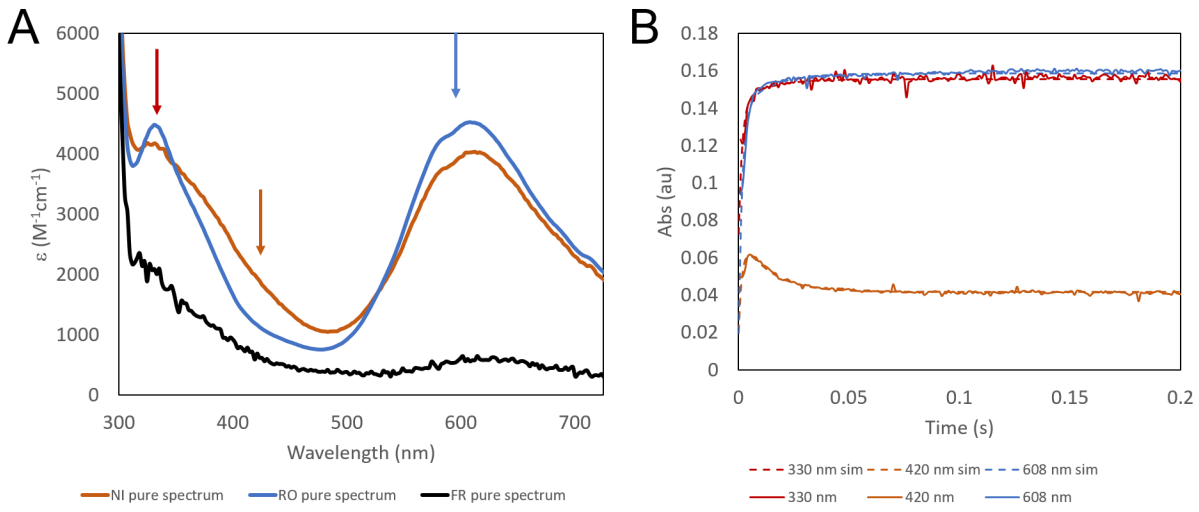

Figure S6: Extracted SVD spectra of RO, NI, and FR (A) and fits to 330, 420, and 608 nm traces (B) of SF Abs data for O_2 reaction with FR Fet3p at pH 7. Data were fit to a model with FR→ NI→ RO with NI decay rates given in Table S3

.

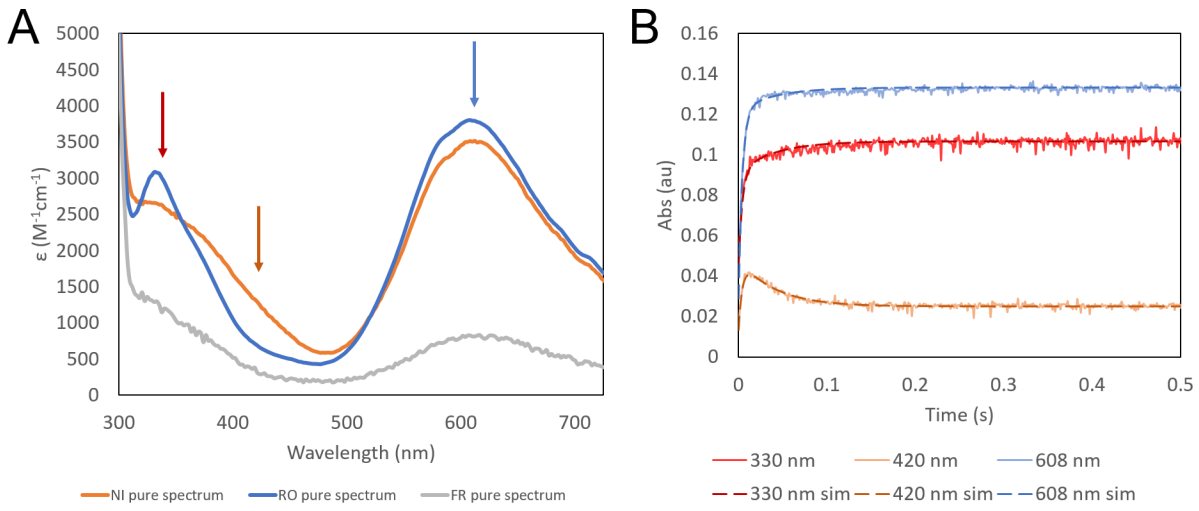

Figure S7: Extracted SVD spectra of RO, NI, and FR (A) and fits to 330, 420, and 608 nm traces (B) of SF Abs data for O_2 reaction with FR Fet3p at pH 7.5. Data were fit to a model with FR→ NI→ RO with NI decay rates given in Table S3

.

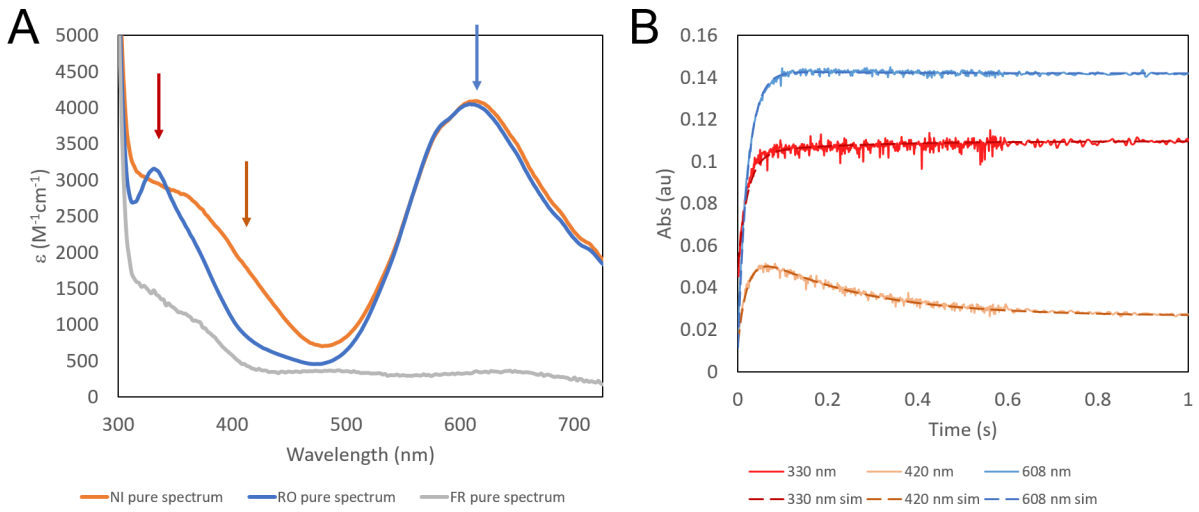

Figure S8: Extracted SVD spectra of RO, NI, and FR (A) and fits to 330, 420, and 608 nm traces (B) of SF Abs data for O_2 reaction with FR Fet3p at pH 8.5. Data were fit to a model with FR→ NI→ RO with NI decay rates given in Table S3

.

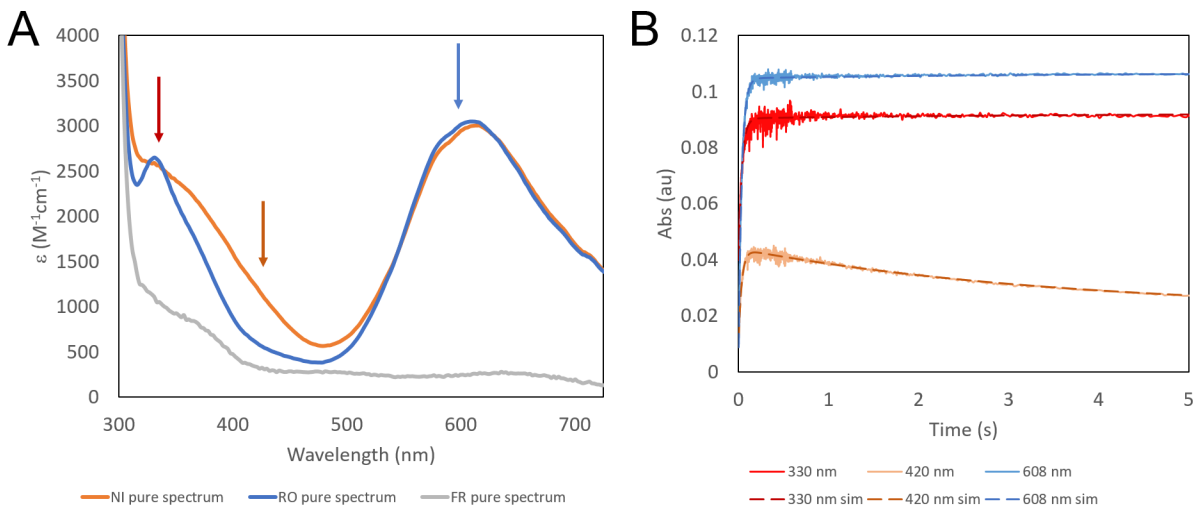

Figure S9: Extracted SVD spectra of RO, NI, and FR (A) and fits to 330, 420, and 608 nm traces (B) of SF Abs data for O_2 reaction with FR Fet3p at pH 9.5. Data were fit to a model with FR→ NI→ RO with NI decay rates given in Table S3

.

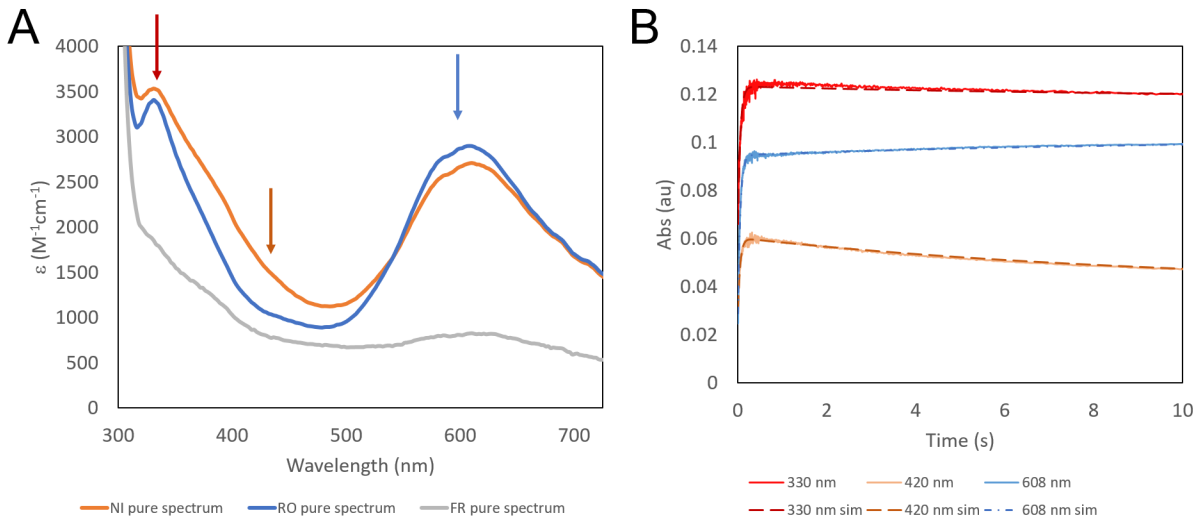

Figure S10: Extracted SVD spectra of RO, NI, and FR (A) and fits to 330, 420, and 608 nm traces (B) of SF Abs data for O_2 reaction with FR Fet3p at pH 10. Data were fit to a model with FR→ NI→ RO with NI decay rates given in Table S3

.

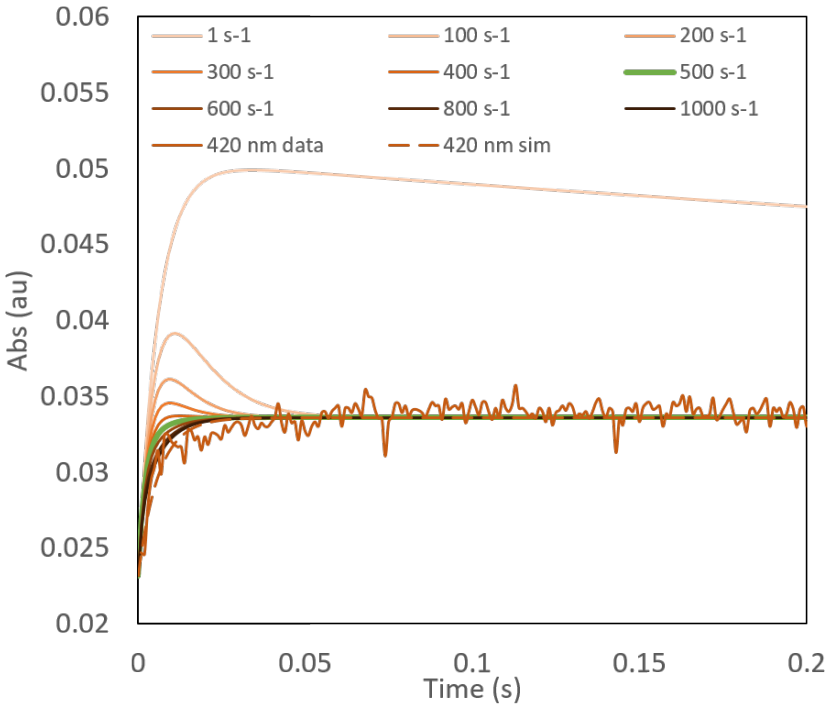

Figure S11: 420 nm Abs trace of pH 6 reoxidation experiment. Dashed line gives simulation from model with no NI formation (as in Figure S5). Simulated 420 nm Abs traces are overlaid with varying NI decay rates between 1 and 1000 s^{-1}. Simulation with NI decay rate of 500 s^{-1} is shown in bold green trace. At rates <500 s^{-1} NI formation and decay behavior is apparent in the simulations.

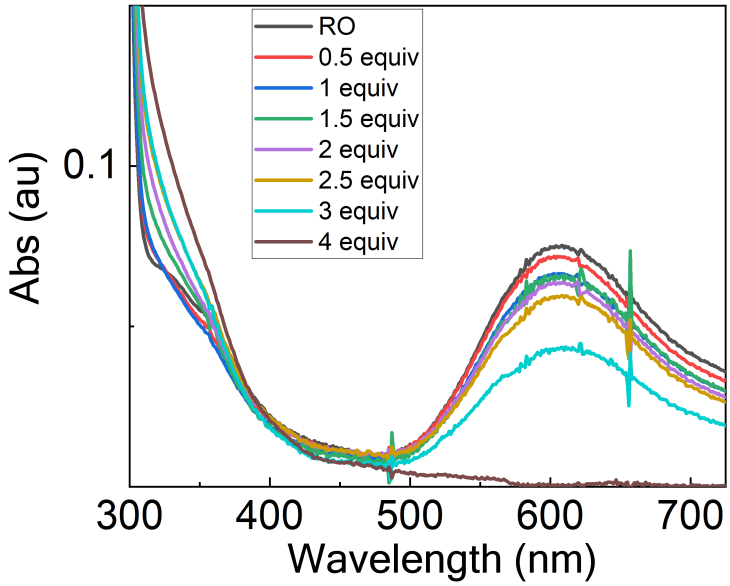

Figure S12: UV-Vis spectra of reduction titration of Fet3p after addition of 0–4 equiv Fe^{II}.

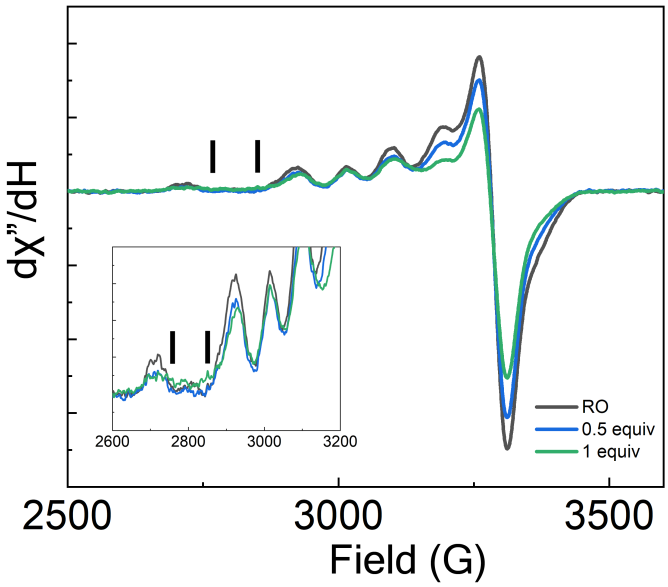

Figure S13: EPR spectra of reduction titration of Fet3p after addition of 0, 0.5, and 1 equiv Fe^{II}. Inset shows enlarged $g_{||}$ region. Black bars indicate location of two low-field T3-HR Cu^{II} hyperfine features.

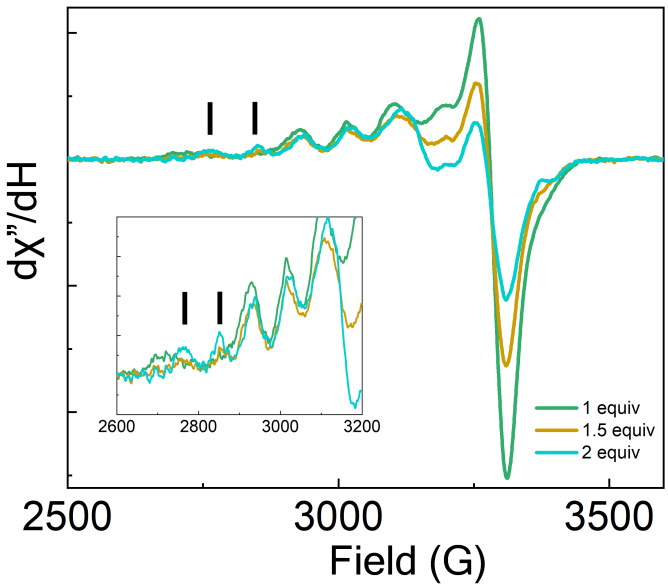

Figure S14: EPR spectra of reduction titration of Fet3p after addition of 1, 1.5, and 2 equiv Fe^{II}. Inset shows enlarged $g_{||}$ region. Black bars indicate location of two low-field T3-HR Cu^{II} hyperfine features.

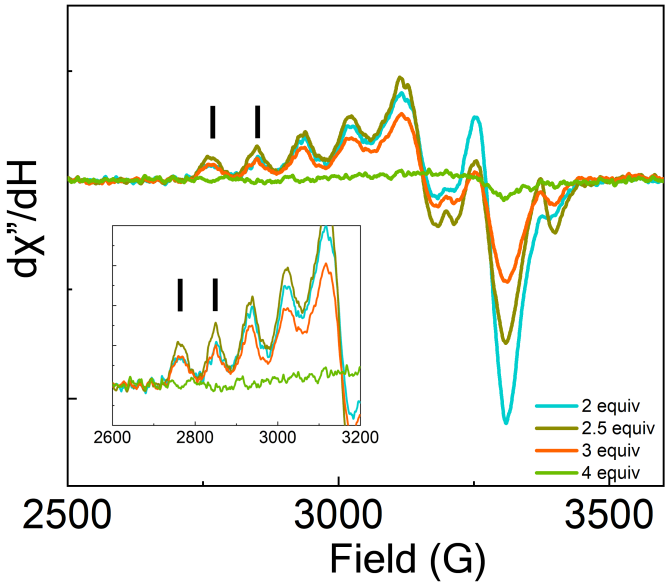

Figure S15: EPR spectra of reduction titration of Fet3p after addition of 2, 2.5, 3, and 4 equiv Fe^{II}. Inset shows enlarged $g_{||}$ region. Black bars indicate location of two low-field T3-HR Cu^{II} hyperfine features.

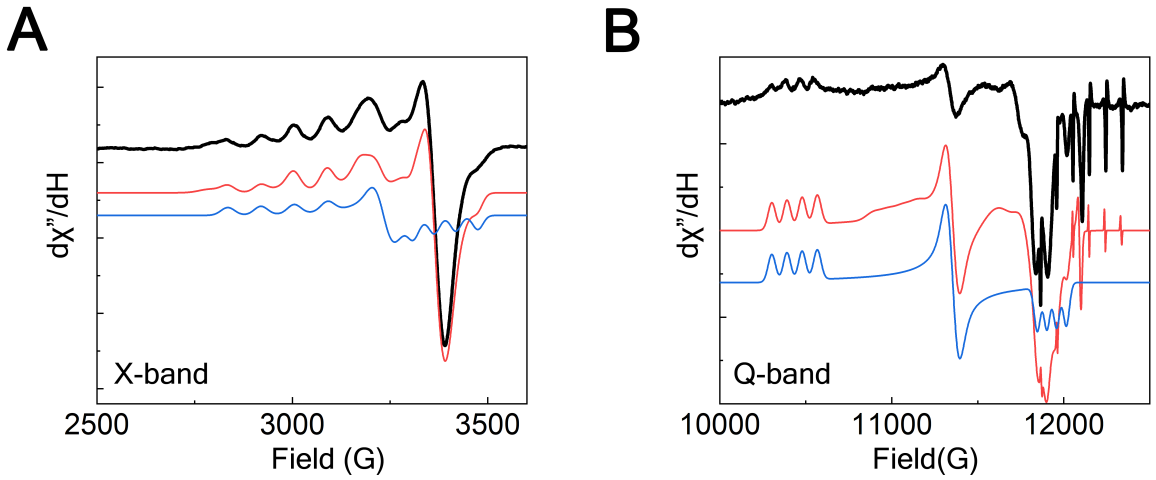

Figure S16: (A) X-band and (B) Q-band EPR spectra of Fet3p treated with 3 equiv Fe^{II} anaerobically. Data plotted in black with simulations of all species present (15% T1, 5% T2, and 80% T3-HR) in red. Simulation of T3-HR only shown in blue. A Mn^{II} impurity from the Q-band EPR tubes is included in the full simulation of B.

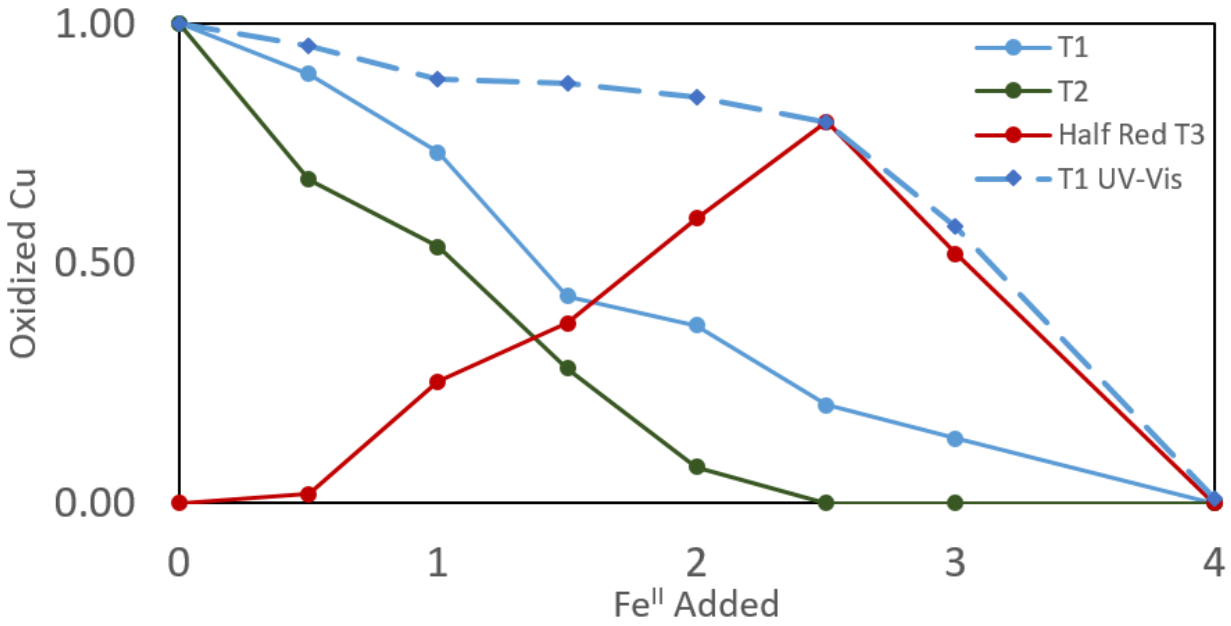

Figure S17: Speciation of T1, T2, and T3-HR species during Fe^{II} titration. Solid lines and points represent EPR data. Dashed line is T1 intensity from UV-Vis

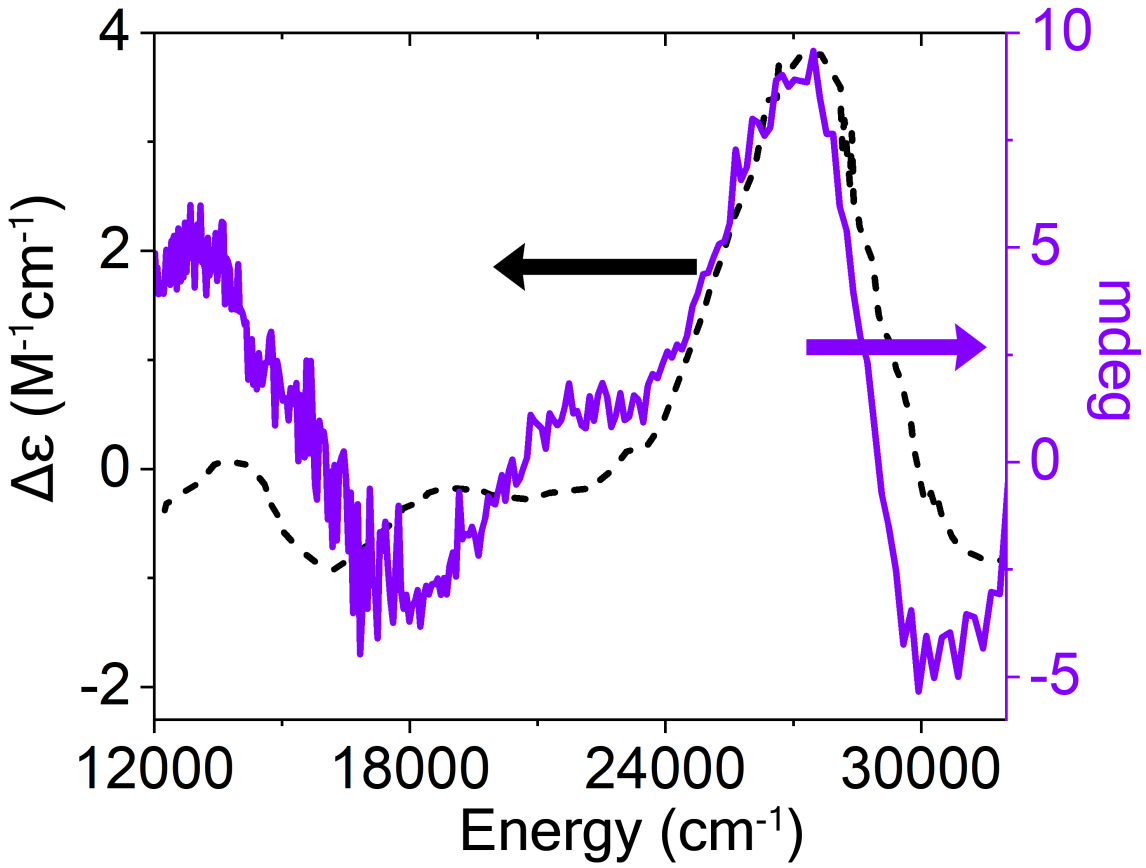

Figure S18: CD spectrum of PI obtained after O_2 reaction with partially reduced Fet3p (purple) overlaid with PI generated from T1D Fet3p (black dashed line) from reference.[1] Colored arrows indicate corresponding axes.

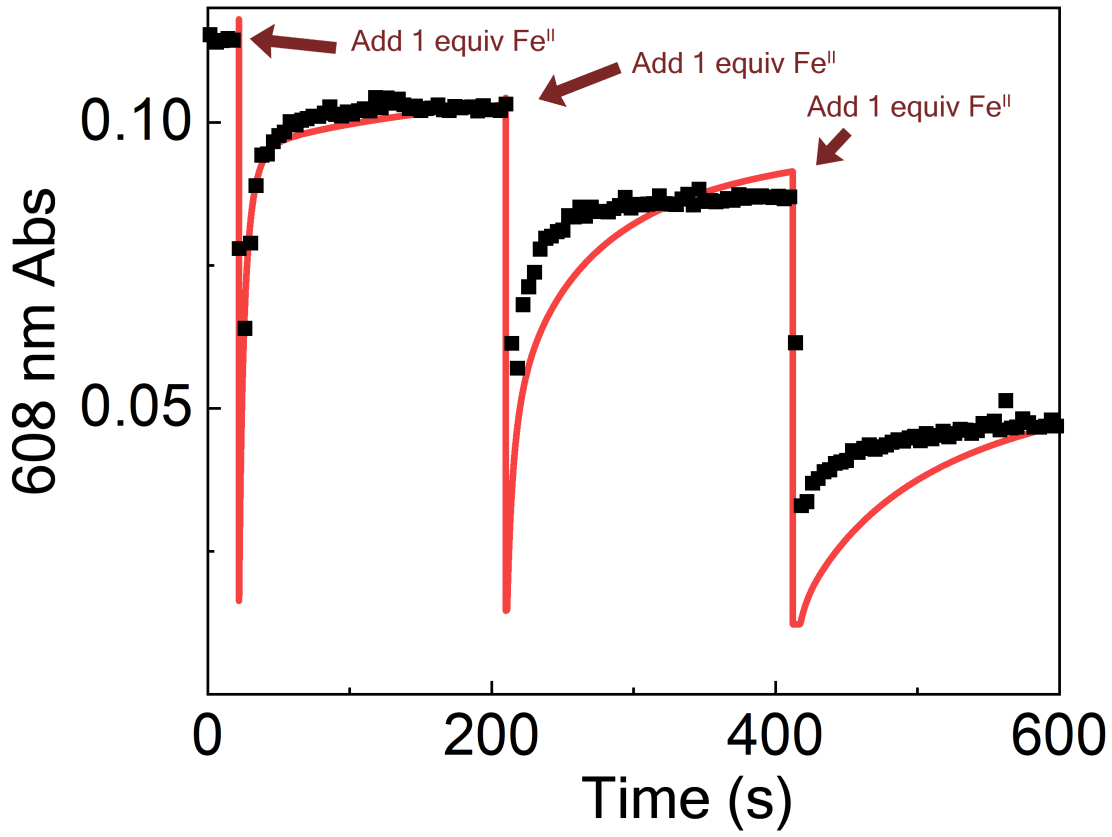

Figure S19: T1 Abs intensity data (black squares) and simulation (red line) of anaerobic RO reduction titration. Stoichiometric amounts of 1, 2, and 3 equiv of Fe^{II} were added to RO Fet3p.

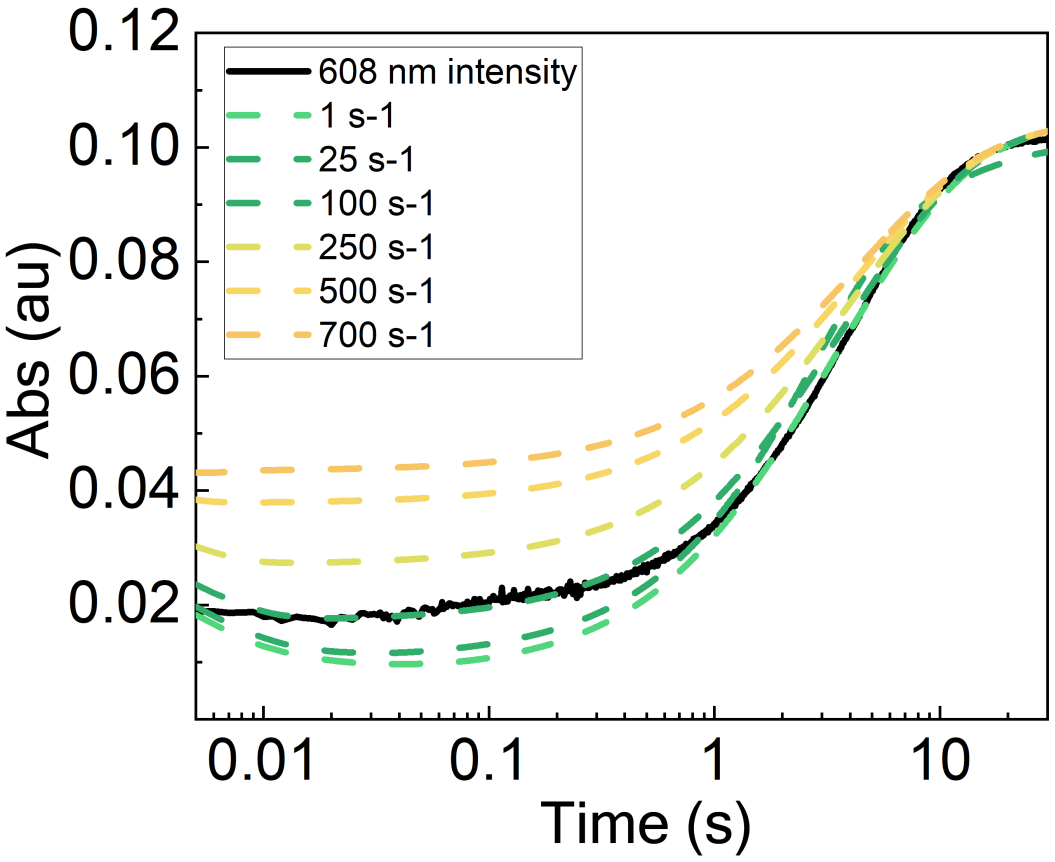

Figure S20: T1 reoxidation following re-reduction of NI Fet3p at pH 6 with different NI reduction rates k_{NI} as labeled.

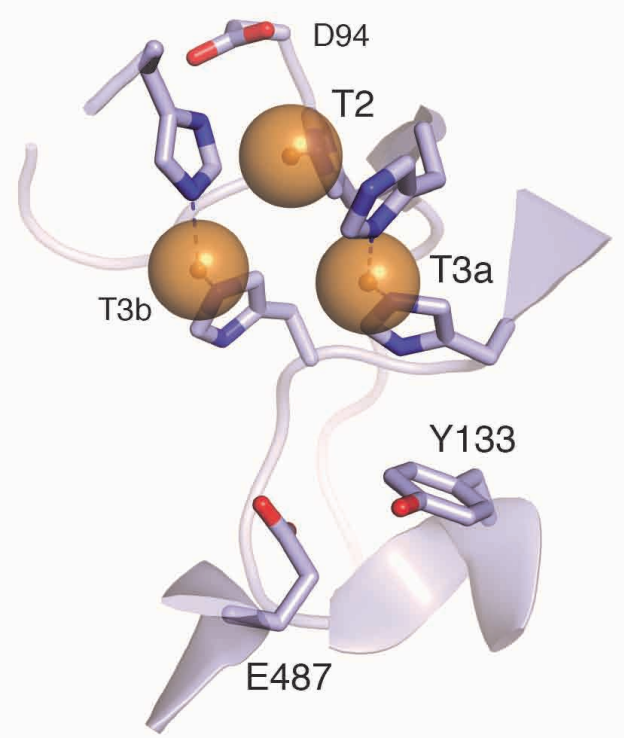

Figure S21: Crystal structure of Fet3p TNC (PDB:1ZPU) showing nearby carboxylic acid residue important for turnover (D94 and E487) and Tyr133 that was mutated to Arg.

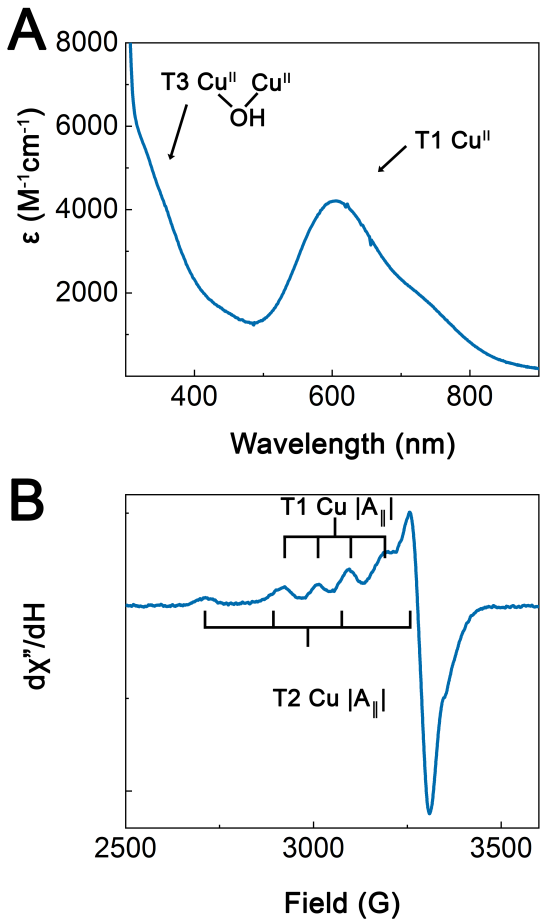

Figure S22: (A) UV-Vis Abs and (B) EPR spectra of Y133R Fet3p.

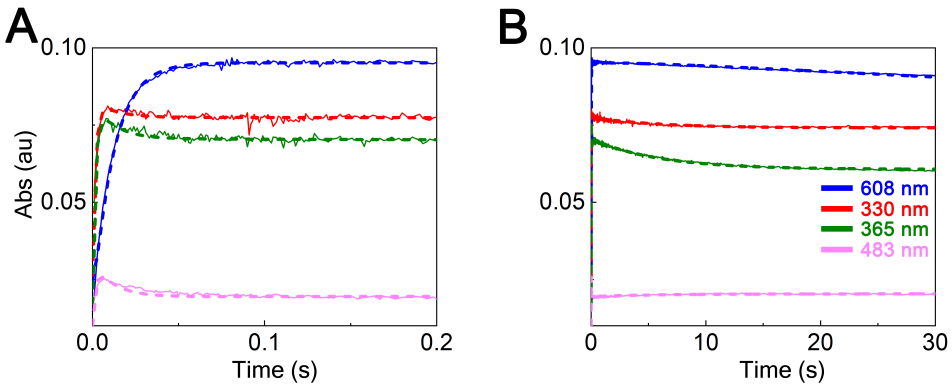

Figure S23: SF Abs traces of O_2 reaction with FR Y133R-Fet3p (pH 7.5, 4 °C). Dashed lines are from simulation according to Scheme 5 with parameters from Table S6

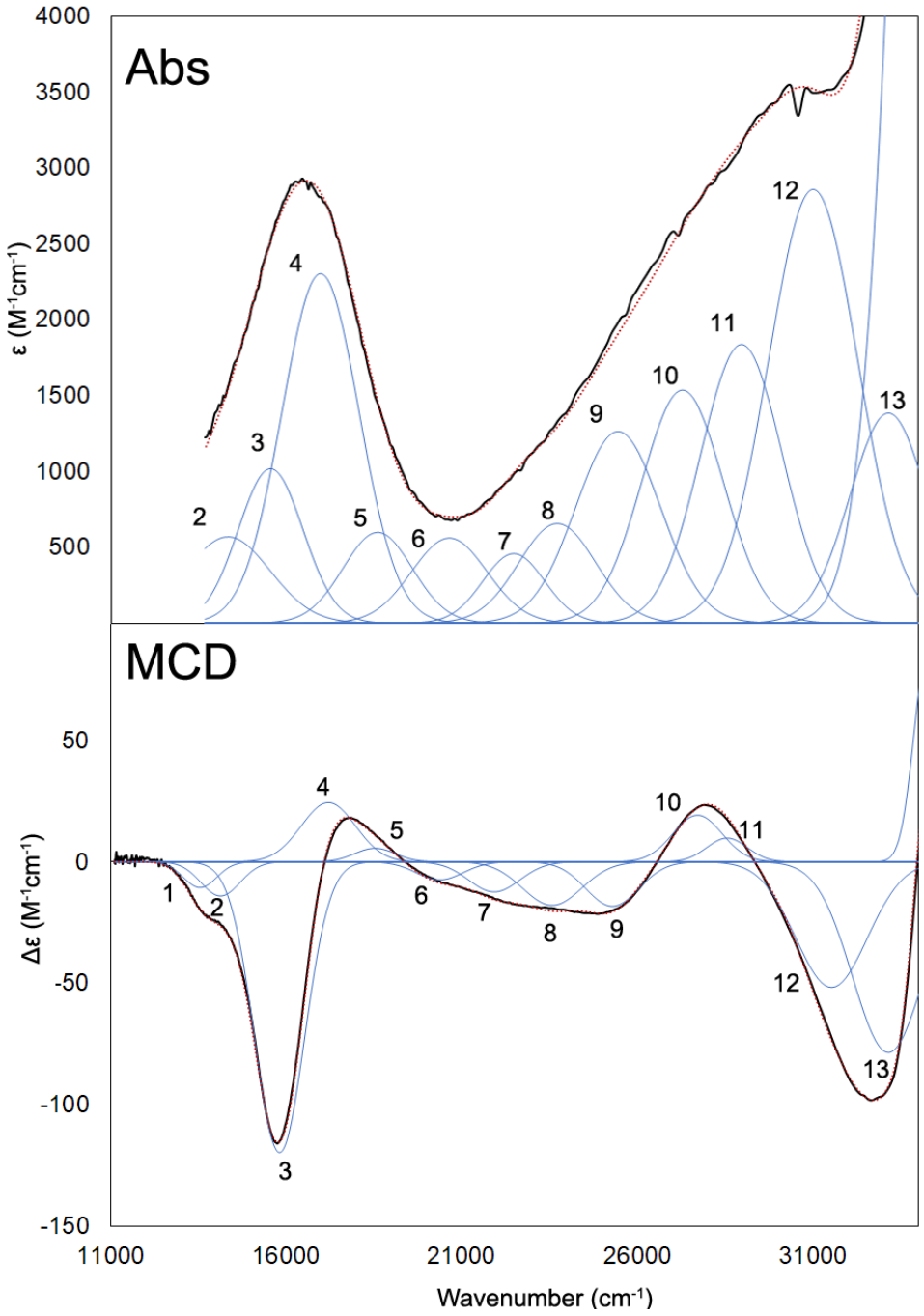

Figure S24: Abs and MCD (4 K, 7 T) spectra of NI in Y133R-Fet3p. Bands 1-13 were simultaneously fit with parameters given in Table S7

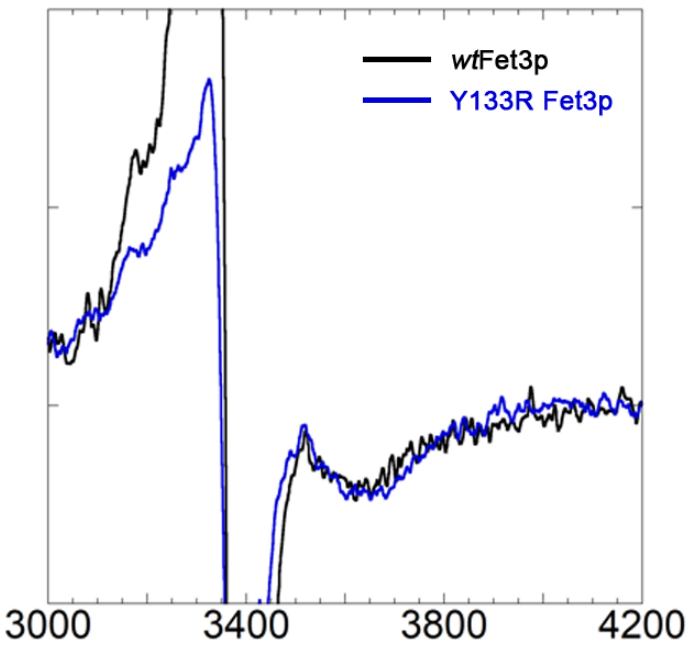

Figure S25: LT EPR (3.8 K, 12.8 mW) spectra of Y133R Fet3p NI (200 ms, pH 6) overlaid with wild-type Fet3p NI (80 ms, pH 8.5). Negative EPR feature is at $g = 1.89$.

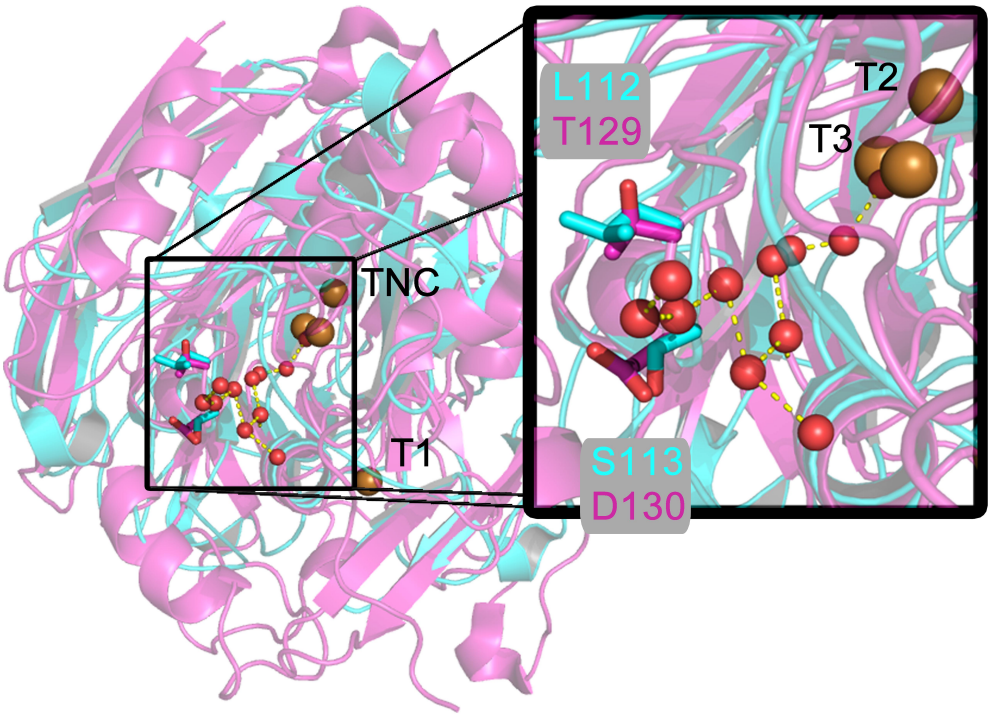

Figure S26: Overlay of *Tv*L (cyan, PDB: 1GYC) and Fet3p (magenta, PDB: 1ZPU) structures showing T1 and TNC Cu's as well as crystallographic water molecules present in *Tv*L structure. Inset shows Leu112 and Ser113 in *Tv*L, which are replaced by Thr129 and Asp130 in Fet3p.

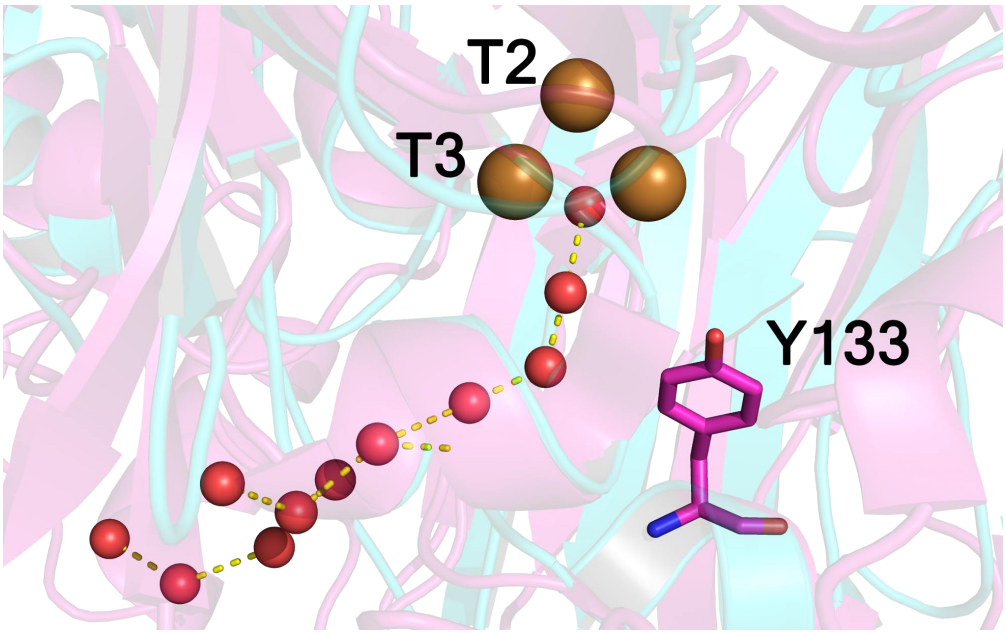

Figure S27: Overlay of *Tv*L (cyan, PDB: 1GYC) and Fet3p (magenta, PDB: 1ZPU) structures showing the Y133 residue, TNC Cu's, and crystallographic water molecules present in *Tv*L structure. The Y133 residue is not part of the crystallographic solvent chain leading to the exterior of the protein.

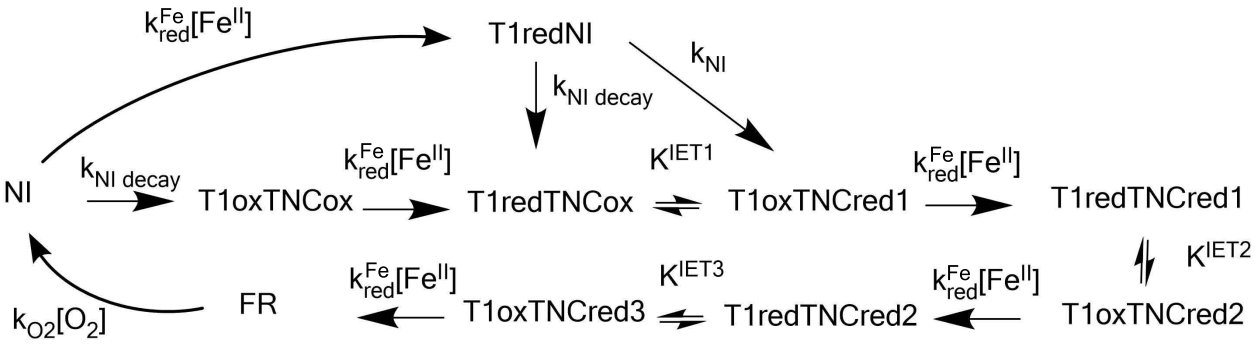

Scheme S1: Fet3p RO and NI Reduction Model

Table S1: Turnover Frequencies for Fe^{II} Oxidation by *wild type* and Y133R Fet3p

Enzyme	TOF (Fe^{II}/s) at 4°C
*wt*Fet3p	0.053(±0.003)
Y133R Fet3p	0.09(±0.02)

Table S2: Spectroscopic Parameters for NI in Wild-Type Fet3p

Band	Assignment	Energy/cm^{-1}
1	T1 d_{xy}	13500(−)
2	T1 d_{yz}	14100(−)
3	T1 d_{xz}	15700(−)
4	T1 Sπ	16900(+)
5	T1 S pseudo-σ	18600(+)
6	His N π	20400(−)
7	His N π	22000(−)
8	His N π	23500(−)
9	NI OH→Cu	25200(−)
10	NI OH→Cu	27600(+)
11	NI OH→Cu	28700(+)
12	NI OH→Cu	31500(−)
13	NI OH→Cu	32800(−)

Table S3: Fet3p NI Decay Rates

pH	$k_{NIdecay}$ (s^{-1})
7	77(±6)
7.5	25(±5)
8.5	4.3(±0.7)
9.5	0.30(±0.05)
10	0.13(±0.02)

Table S4: T3-HR Cu^{II} EPR Parameters

g	$\lvert A_{\parallel}\rvert$ ($\times 10^{-4}$cm^{-1})
2.329	90
2.137	2
2.033	51

Table S5: Speciation of Cu Centers During Fe^{II} Titration

Fe^{II} added	T1ox	T2ox	T3ox
0	1	1	1
0.5	0.95	0.67	0.94
1	0.88	0.53	0.79
1.5	0.88	0.28	0.67
2	0.85	0.07	0.54
2.5	0.79	0	0.35
3	0.58	0	0.21
4	0	0	0

Table S6: Y133R Fet3p PI and NI Decay Rates

pH	PI Decay Rate (s^{-1})	NI Decay Rate (s^{-1})
6	110($\pm$10)	0.14($\pm$0.04)
7.5	88($\pm$4)	0.18($\pm$0.03)
8.5	75($\pm$5)	0.11($\pm$0.04)
9.5	23($\pm$5)	0.09($\pm$0.03)

Table S7: Spectroscopic Parameters for NI in Y133R-Fet3p

Band	Assignment	Energy/cm^{-1}
1	T1 d_{xy}	13500 (-)
2	T1 d_{yz}	14300 (-)
3	T1 d_{xz}	15500 (-)
4	T1 Sπ	17000 (+)
5	T1 S pseudo-σ	18600 (+)
6	His N π	20600 (-)
7	His N π	22500 (-)
8	His N π	23700 (-)
9	NI OH$\rightarrow$Cu	25400 (-)
10	NI OH$\rightarrow$Cu	27300 (+)
11	NI OH$\rightarrow$Cu	29000 (+)
12	NI OH$\rightarrow$Cu	31000 (-)
13	NI OH$\rightarrow$Cu	33200 (-)

References

(1) Palmer, A. E.; Quintanar, L.; Severance, S.; Wang, T. P.; Kosman, D. J.; Solomon, E. I. Spectroscopic characterization and O2 reactivity of the trinuclear Cu cluster of mutants of the multicopper oxidase Fet3p. *Biochemistry* **2002**, *41*, 6438–6448.